ACS APPLIED MATERIALS & INTERFACES

Research Article

www.acsami.org

Highly Flexible, Multipixelated Thermosensitive Smart Windows Made of Tough Hydrogels

Thanh-Giang La,[†,‡,§,#] Xinda Li,[†,#] Amit Kumar,[†] Yiyang Fu,[∥] Shu Yang,[⊥] and Hyun-Joong Chung*[,†]

[†]Department of Chemical and Materials Engineering, University of Alberta, Edmonton, Alberta T6G1H9, Canada

[‡]Institute for Reconstructive Sciences in Medicine (iRSM), Misericordia Community Hospital, Edmonton, Alberta T5R4H5, Canada

[§]Department of Communication Sciences and Disorders, University of Alberta, Edmonton, Alberta T6G2G4, Canada

[∥]Department of Electrical and Computer Engineering, University of Alberta, Edmonton, Alberta T6G1H9, Canada

[⊥]Department of Materials Science and Engineering, University of Pennsylvania, Philadelphia, Pennsylvania 19104, United States

Supporting Information

ABSTRACT: In a cold night, a clear window that will become opaque while retaining the indoor heat is highly desirable for both privacy and energy efficiency. A thermally responsive material that controls both the transmittance of solar radiance (predominantly in the visible and near-infrared wavelengths) and blackbody radiation (mainly in the mid-infrared) can realize such windows with minimal energy consumption. Here, we report a smart coating made from polyampholyte hydrogel (PAH) that transforms from a transparency state to opacity to visible radiation and strengthens opacity to mid-infrared when lowering the temperature as a result of phase separation between the water-rich and polymer-rich phases. To match a typical temperature fluctuation during the day, we fine-tune the phase transition temperature between 25 and 55 °C by introducing a small amount of relatively hydrophobic monomers (0.1 to 0.5 wt % to PAH). To further demonstrate an actively controlled, highly flexible, and high-contrast smart window, we build in an array of electric heaters made of printed elastomeric composite. The multipixelated window offers rapid switching, ∼70 s per cycle, whereas the device can withstand high strain (up to 80%) during operations.

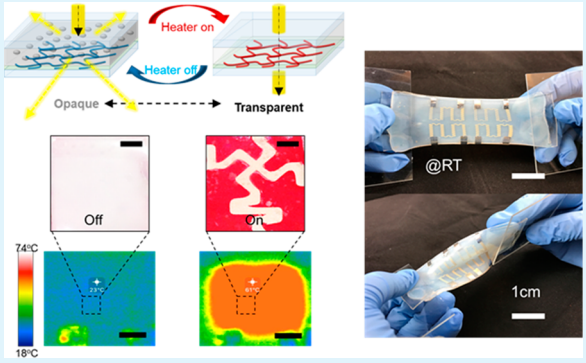

KEYWORDS: *tough hydrogels, smart windows, optical coating, stretchable electronics, phase separation*

INTRODUCTION

Materials that can switch light absorption, scattering, and transmission properties in response to external stimuli offer new mechanisms to create smart windows for privacy, comfort, and energy efficiency.[1−3] The switching is typically triggered by electric field (e.g., electrochromic,[4] crystalline phase control,[41] etc.) or light intensity (photochromic).[4] For example, electrochromic materials applied as a thin coating in smart windows change the oxidation states as a function of the applied electric field, which in turn modulates the optical properties of the layer.[5,6] However, it requires continuous operations of such windows under the field, which is not energy efficient; in addition there are the issues of cost and long-term stability of the electrochromic materials. Therefore, a smart window that can passively modulate its transparency as a function of the environmental temperature (i.e., thermochromic) is highly desired for energy-saving operations.[7] For example, one can design a smart window that can take advantage of the solar radiation (typically 0.3−2 μm in wavelength) into the building when the outside is cold, but block it when it is scorching hot. Metal oxide nanoparticles, such as vanadium oxide (VO_2) that has been utilized in electrochromic smart windows,[7] is extensively explored as a potential candidate material for this purpose. In addition, the thermochromic VO_2-based thin films can block near-infrared light at temperatures >40 °C, and thus can save energy for air conditioning in hot weather.[8,9] However, it remains challenging to balance the useful transition temperature and the degree of transparency change.[2,10,11] Another drawback of oxides is that they require a tightly sealing encapsulation layer to prevent oxidation from the environment,[12−14,34] which will change the optical properties, thus limiting the fitting and sizing of such smart windows for different built structures.

Recently, it has been shown that simply stretching and releasing a composite elastomer film offer a dramatic change in optical transmittance in the visible wavelength range.[15,16] It is also possible to achieve a fast response (∼15 s/half of cycle) by stretching porous elastomers consisting of a surface-infused

Received: June 20, 2017
Accepted: August 24, 2017
Published: August 24, 2017

DOI: 10.1021/acsami.7b08907
ACS Appl. Mater. Interfaces 2017, 9, 33100−33106

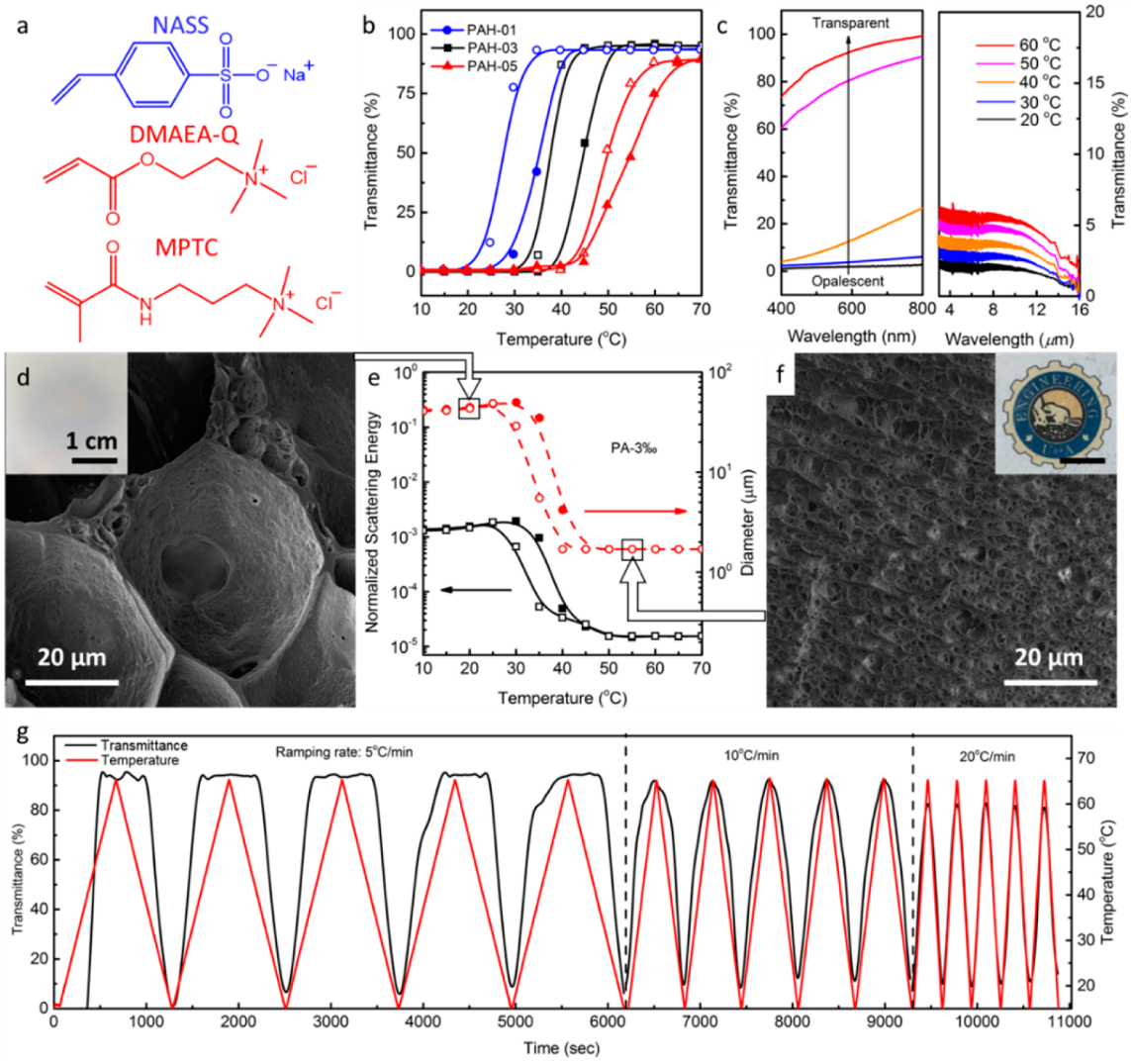

Figure 1. (a) Monomers used in the synthesis of polyampholyte hydrogels (PAHs). (b) Optical transmittance (635 nm incidence beam through 0.5 mm PAH films) as a function of temperature for PAH-01 (blue circle), PAH-03 (black square), and PAH-05 (red triangle). Open and closed symbols represent cooling and heating cycles, respectively. Transmittance of the PAH-03 film with respect to electromagnetic wavelength at different temperatures (c) in the optical range (left, visible to near-IR) and in the thermal radiation range (right, mid-IR). Cross-section SEM images of freeze-dried PAH-03 (d) at 20 °C and (e) at 55 °C quenched in the liquid nitrogen. The insets are photographs of the U of A Engineering logo coated with the PAH-03 film at the respective temperatures (opalescent at 20 °C and transparent at 55 °C). Logo reproduced with permission. Copyright Faculty of Engineering at the University of Alberta. (f) Normalized scattering energies (635 nm laser beam through the PAH-03 film) and respective size of microstructure objects (modeled as the diameters of spheres) as functions of temperature. (g) Dynamic optical response of PAH-03 to three temperature ramp rates of 5, 10, and 20 °C/min.

liquid.[17] Here, we exploit temperature induced phase separation in tough hydrogels to create thermosensitive smart windows, whereas the elastomeric nature of the hydrogel films offers morphological flexibility in fitting variably sized windows.

Hydrogels or ionogels can contain a large amount of liquid in the polymer network while allowing for mechanical deformation without leakage. Recently, poly(*N*-isopropylacrylamide) (PNIPAAm) hydrogel has drawn much attention due to its unique combination of stretchability and thermochromism (e.g., vanadium dioxide, VO_2).[18−22] Specifically, it undergoes a transition from transparency to an opaque state upon heating above the lower critical solution temperature (LCST, ∼32 °C), which is suitable for the smart window application.

Recently, Kodak Research Laboratories blended a small fraction of PNIPAAm as a nanoscopic aggregation in a self-healing gel matrix to achieve rapid switching from transparency to opalescent states within ∼30 s.[22] It is noted that most synthetic hydrogels, including PNIPAAm, are intrinsically brittle and their mechanical integrity of such a layer over time is of concern. Therefore, development of a tough hydrogel that can overcome such limitations will allow us to achieve superb tear-resistance, stretchability, and self-healing ability.[23−25,27,28]

Polyampholyte hydrogels (PAHs), where the polymer networks are associated by ionic bonding between oppositely charged units in their backbone chains, are intrinsically tough, stretchable, and self-healing.[28] They have been used as absorbents in wastewater metal removal,[29] tissue adhesives,[30] and electrolytes for supercapacitors.[31] PAH exhibits a reversible optical transition from opaqueness to transparency upon heating above the upper critical solution temperature (UCST).[32] This is because water and the polymer chains

DOI: 10.1021/acsami.7b08907
ACS Appl. Mater. Interfaces 2017, 9, 33100−33106

phase-separate at the temperatures below UCST to form macroscopic water-rich and polymer-rich domains. As Mie's theory states, the larger macroscopic water-rich domains scatter electromagnetic light to provide optical opaqueness; meanwhile, the smaller ones, or even a homogeneous medium, transmit most of light as transparent.

In this work, we introduce a new design of a thermosensitive smart window based on PAH. At a high temperature (i.e., during the day), our PAH is transparent so that visible light can transmit. At a lower temperature (i.e., at night), our PAH blocks the visible light, and the transmittance of mid-infrared (mid-IR) radiation (3−40 μm in wavelength, corresponding to the blackbody radiation at an ambient temperature) also decreases. Blackbody radiation through a window is a significant source of heat loss from a building.[33] Accordingly, our PAH-based smart windows operate like regular windows during daytime with high transparency, but become opaque at nighttime, allowing for privacy, and, more importantly, heat retention within the residence. By adjusting the monomer compositions in PAH gel (i.e., molecular doping), we fine-tune UCST between ∼25 and ∼55 °C to reflect the typical daily temperature fluctuation within a building. Further, we fabricate a proof-of-concept, multipixel *active* smart window by integrating an array of stretchable heaters and with the PAH layer encapsulated by acrylic elastomers. The PAH conforms and adheres to the contour of various elastomer sheets when subjected to a large degree of stretching and twisting.

RESULTS AND DISCUSSION

Controlling Cloud Points of the PAH. The PAH was synthesized from a precursor solution consisting of an anionic monomer (sodium 4-vinylbenzenesulfonate, NaSS), two cationic monomers {[2-(acryloyloxy)ethyl]-trimethylammonium chloride, DMAEA-Q, and (3-(methacryloylamino)propyl)trimethylammonium chloride, MPTC (Figure 1a)}, with a cross-linker (*N*,*N*′-methylenebis-(acrylamide), MBAA) and a photoinitiator (2-oxoglutaric acid). After photo-cross-linking under UV light, the resulting PAH, poly(DMAEA-Q-*co*-NaSS-*co*-MPTC), with thickness of 0.5 mm was stretchable yet tough. All PAHs mentioned in this study were charge-balanced (i.e., consisting of the same amount of anionic and cationic monomers). In addition, the monomer conversion rate of the resulting PAH was examined by nuclear magnetic resonance spectroscopy (i.e., ^{1}H NMR spectroscopy, see Figure S5, Supporting Information). Previously, PAH made from NaSS and DMAEA-Q without MPTC exhibited a cloud point of ∼15 °C.[32] Here, by introducing a small quantity (≤0.5 wt %) of a more hydrophobic monomer, MPTC, we increased the cloud point of PAHs. We refer to this procedure as molecular doping. Our nomenclature of PAH-0*x* indicates that 0.*x* wt % of DMAEA-Q is replaced with MPTC with respect to the molar concentration of total cationic species. Figure 1b shows a drastic transition of visible light transmittance for PAH-01, PAH-03, and PAH-05 with respect to temperature. UCST increased with increasing MPTC content. Here, the driving force for phase separation is attributed to the hydrophobic effect, and thermal energy is needed for water molecules to break the hydrophobic interactions between the polymer chains to form a homogeneous, one-phase structure.[35−37] Hysteresis between heating and cooling curves was visible (∼6 °C in width for stepwise leveled-up temperature with an interval of 5 °C in 10 min).

The two panels in Figure 1c represent the transmittance of light (visible to near-IR; left panel) and thermal radiation (mid-IR; right panel) through PAH-03 (0.5 mm thick). Below UCST, the transmittance values of light range were <1% at 20 °C and <10% at 30 °C, respectively. Above the cloud point, homogenized PAH-03 transmitted a significant amount of the electromagnetic wave: from 60% (400 nm) to 82% (800 nm) at 50 °C and from 74% (400 nm) to 95% (800 nm) at 60 °C. Consequently, the PAH-03 switched from optically opalescent to transparent from 20 to 60 °C (see insets in Figure 1d,f). PAH-03 contained 72.1 ± 4.7 wt % of water, which is known for a high level of absorption for mid-IR radiation. Hence, less than 7% mid-IR radiation (3−16 μm) was transmitted at 20 °C and less than 2% at 60 °C.

Phase Separation and Structure of PAH-03. We then investigated the light scattering of the phase-separated domains (wavelength, 635 nm; incidence angle, 75°). Figure 1e shows the normalized scattering intensity, which is the light intensity measured at the detector divided by the incidence laser intensity (see experimental setup in Figure S1, Supporting Information), measured at temperatures between 10 and 70 °C. As the temperature increased, the scattering intensity (black squares and solid lines) underwent a 2-order-of-magnitude decrease from 2×10^{-3} (at 20 °C) to 1.2×10^{-5} (at 55 °C). The decrease in scattering intensity at the higher temperature is attributed to the reduced size of water-rich domains. Scanning electron microscope (SEM) images of freeze-dried PAH-03 captured the morphology of polymeric networks at 20 °C (Figure 1d) and at 55 °C (Figure 1f), respectively. A piece of PAH-03 sample was kept at 20 °C, and another was heated to be at 55 °C for 5 min; both were quenched in liquid nitrogen immediately to preserve the polymer structures in the hydrogel. At 20 °C, bubblelike porous structures (∼40 μm in diameter) were observed, representing the macroscopic phase-separated water-rich domains. In contrast, the 55 °C sample appeared to have much smaller (∼1 μm) and more homogeneously porous structures. In addition, a differential scanning calorimetry (DSC) measurement was acquired for the PAH-03 at temperatures between 15 and 65 °C (see Figure S4a, Supporting Information). A phase transition of PAH-03 indicated by DSC measurement was observed at 43.4 °C (heating) and 38.9 °C (cooling), values that were close to the apparent cloud point in Figure 1b, as determined by the first-order derivative of the transmittance of PAH-03 (Figure S4b,c, Supporting Information).

The size of the water-rich domains was further deduced from the scattering intensity values in Figure 1e. Following the Mie scattering theorem by approximating the water-rich domains as spherical objects, the scattering light intensity I_{sca} can be quantitatively predicted by[38]

$$I_{sca} = \frac{I_0 \lambda^2}{8\pi^2 r^2}[i_1(\theta) + i_2(\theta)] \quad (1)$$

where I_0 is the incident intensity, r is the spherical radius of the domains, λ is the wavelength of light, θ is the scattering angle, and (i_1, i_2) are the intensity functions of Mie scattering. The calculated r values are shown in Figure 1e (red circles; dotted lines are a guide to the eye). The calculated domain size agrees well with the results from SEM (Figure 1d,f) and optical images (Figure 1b−d (inset) and f (inset)), confirming UCST between 30 and 40 °C for PAH-03.

DOI: 10.1021/acsami.7b08907
ACS Appl. Mater. Interfaces 2017, 9, 33100−33106

Dynamic Optical Response of PAH-03. The transmittance of PAH-03 at 635 nm was measured continuously under the programmed heating and cooling cycles between 15 and 65 °C at the ramping rates of ±5, ±10, and ±20 °C/min (Figure 1g). The triangular functions for temperature control have periods of 20, 10, and 5 min, respectively. The PAH-03 film demonstrated optical contrast values of 85%, 78%, and 67%, respectively. The transitions from opalescence to transparency and vice versa were reversible without any noticeable degradation throughout our measurement for more than 100 cycles, which is expected from the phase separation mechanism.

Fabrication of an Active Smart Window. The thermosensitive PAH can be utilized in passive smart window applications. Here, we further exploit the precise control of temperatures using an integrated array of printed heaters beneath the PAH layer for active switching. In order to keep the merit of PAH as a flexible optical coating material, which will allow easy sizing and fitting into any existing windows, all components in the active device, including the heater and encapsulation layers, are made of elastomeric materials.

Figure 2a illustrates different layers in the active smart window device. Fluoroelastomeric conducting ink developed in our lab[39] was 3D printed (nozzle diameter of 200 μm) on an elastomeric polydimethylsiloxane (PDMS) film (0.1 mm thick), which served as the flexible and stretchable heater layer. In our study, the conductive ink showed resistivity of 1.17×10^{-3} Ω cm at room temperature. The printed region with a cross-sectional area of 9×10^3 μm^2 functioned as a Joule heater when passing a large current. The PAH-03 layer was responsible for the optical switching.

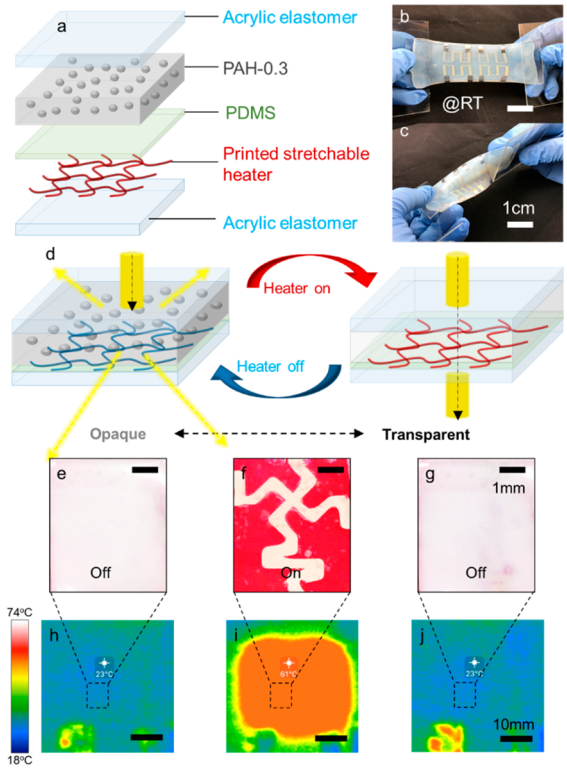

Figure 2. (a) Illustration of the individual layers in the active smart window using 0.5 mm thick PAH-03 as an optically functional medium. Top views of the smart window at (b) uniaxially stretched and (c) twisted modes of deformation. (d) Schematic of transparency control of the window by supplying direct current to the printed elastic heater. Simultaneously taken (e–g) optical and (h–j) thermogram images of the device under operation (25 and 45 s for heating and cooling, respectively).

An issue of hydrogel-based materials is the drying-out of water over prolonged operation time, leading to delamination and stability issues. This concern needs to be addressed especially for thermally activated devices. A previous study by Zhao's group addressed the issue by encapsulating hydrogels in elastomers.[40] In our work, the trilayer device (PAH-03/PDMS/heater) was sandwiched between two layers of commercially available acrylic elastomer, VHB 4905 (3M). VHB is known for high deformability and can form strong adhesion with various electrode materials, including graphene[41] and hydrogel-based ionic conductors.[26,42] In our work, the VHB film offered a moderate adhesion to the hydrated PAH-03 and prevented the drying of water from the hydrogel. Overall, our device was inherently stretchable with each layer adhered to the other. Consequently, the fabricated device could operate under highly deformed conditions, as evidenced by Figure 2b (uniaxial strain up to 80%) and Figure 2c (twisting deformation). Figure 2d illustrates the operation of the active smart window, where the current input through the printed heater modulated the smart window's optical transparency. The adhesion between both elastomer layers (PDMS and VHB) and PAH-03, however, weakened after 3 days under the ambient condition, causing delamination at the interface. Long-term adhesion between the hydrogel and the elastomers will be essential to repeated device operations. It has been shown that tough hydrogels can be chemically anchored on the surface of PDMS,[40−44] which may shed light on addressing this issue.

Operation of the Active Smart Window. Figure 2h–j shows snapshots of measured hydrogel temperature evolution over a wide area. Figure 2e–g (and Video S1, Supporting Information) shows optical images of a selected spot. At rest, the window was opalescent (Figure 2e), and the measured temperature was 23 °C (Figure 2h). Upon heating with 0.5 A for 25 s, the *whole* pixel area became optically transparent (Figure 2f) while the temperature was equilibrated at 61 °C (Figure 2i). After removal of the current input for 45 s, the window went back to *complete* opalescence (Figure 2g), while most of the area was cooled down to 23 °C within the short period of time (Figure 2j). The complete switching cycle took 70 s, which is comparable with the fastest switching speed reported in the literature (see Table S1, Supporting Information).

Figure 3 shows the electro-thermal behavior of the elastic heater, operating under a uniaxial tensile strain of 50%. Here, the smart window was stretched to demonstrate its flexibility of operation under deformation. We note that the switching mechanism is not related to the deformation. Figure 3a,b shows the thermal response of the heater under a pulse wave of alternating 0 to 0.5 A for >1000 cycles over more than 10 h. The period of the rectangular function was 36 s (18 s each for heating and cooling). Here, the resistance value can be directly converted to the temperature of the heater by using the measured temperature coefficient of our heater material, 4.8×10^{-3}/°C (Figure 3d was converted to Figure 3i). The resulting temperature distribution in the on and off states was measured by an IR camera from the heater's side and hydrogel's side, respectively (Figure 3e–h). The hydrogel side achieved a uniform temperature of ∼60 °C by input of a current of 0.5 A for only 18 s. After removal of the current for 18 s, the hydrogel

DOI: 10.1021/acsami.7b08907
ACS Appl. Mater. Interfaces 2017, 9, 33100−33106

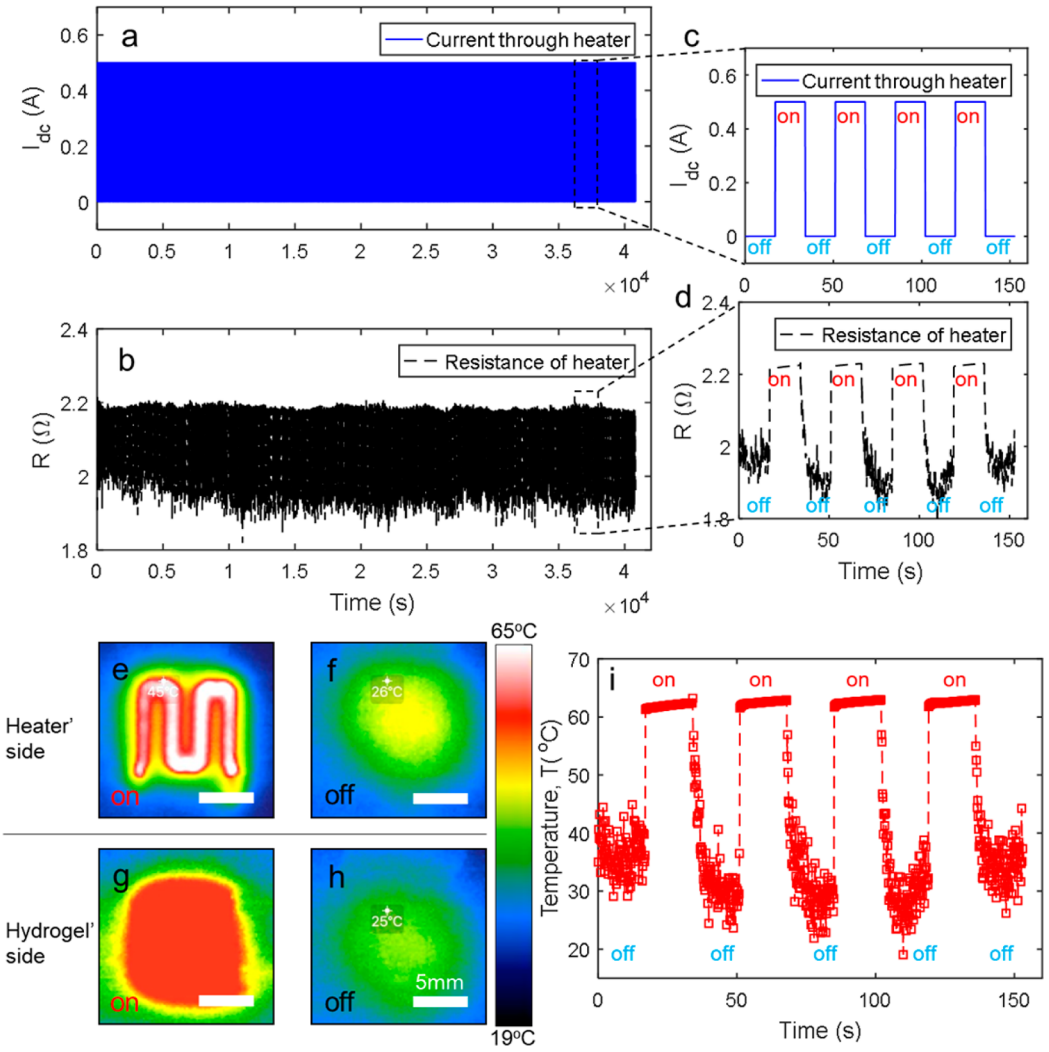

Figure 3. Time history of the applied current over (a) ~1000 cycles, (b) 4 cycles after 10 h. Measured resistance of (c) ~1000 cycles, (d) 4 cycles after 10 h of the heater in response to the cyclic current application. Thermograms recorded by a thermal infrared camera: on the heater's side activated by (e) 0.5 A (on) and (f) 0 A (off); on the hydrogel's side activated by (g) 0.5 A (on) and (h) 0 A (off). (i) Calculated temperature of the heater by corresponding to its resistance value with a temperature coefficient of 4.8 × 10^{-3}/K (see Figure S2, Supporting Information).

film was cooled down to nearly ambient temperature. It should be noted that this time duration does not refer to the speed of optical switching to the level of ~100% transmittance contrast as indicated in Figure 1b.

We further designed a 2 × 2 array pixelated active smart window. As seen in Figure 4a–d, and Videos S2 and S3 in the Supporting Information, optical and thermal transparency can be individually controlled by the geometry of the embedded heaters. In future works, such a device can be further optimized by employing transparent heater materials.

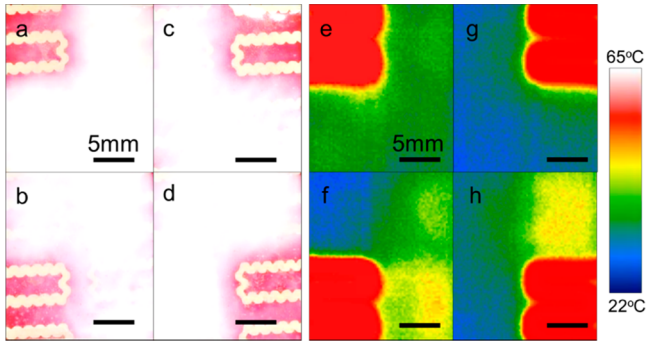

Figure 4. (a–d) Optical photographs of the device under pixelated control. (e–h) Thermograms of the heaters under pixelated activation.

CONCLUSION

In summary, we developed a flexible smart window from a polyampolyte hydrogel showing 80% in transmittance contrast from opalescence (at a low temperature) to transparency (at a high temperature), which could undergo a large deformation (up to 80% strain). The phase transition temperature of the polyampolyte hydrogels could be fine-tuned by molecular doping of a small amount of hydrophobic monomers into cationic monomers. By printing a stretchable elastic heater layer onto the hydrogel film, we demonstrated a pixelated array of actively tunable smart windows. The thermosensitive smart window we develop can be both passive and active, allowing for applications in different operation conditions. Our window is highly robust against large deformation, a characteristic not possible with a glass window and yet offering a fast switching speed. We believe the study presented here will offer new insights to design smart windows that can not only change

DOI: 10.1021/acsami.7b08907
ACS Appl. Mater. Interfaces 2017, 9, 33100–33106

optical transparency but also retain indoor heat at night. Future work is needed to study the IR reflection of PAH, as well as tunability of mid-IR in response to temperature for the energy-saving aspect.

METHODS

PAH Synthesis. To prepare polyampholyte hydrogels (PAHs), we followed Gong and co-workers' protocols for an one-step random copolymerization.[28] NaSS, MPTC, DMAEA-Q, MBAA, and 2-hydroxy-4′-(2-hydroxyethoxy)-2-methylpropiophenone (photoinitiator) were purchased from Sigma-Aldrich and used as received. The aqueous solution of 1 M NaSS, (1−x) M DMAEA-Q, x M MPTC, 2 mM MBAA, and 1 mM photoinitiator was injected into a cell consisting of two glass plates using a Teflon spacer (thickness 0.5 mm). Here, the x values were between 0.001 and 0.005. For the characterizations of optical properties of PAHs, no PDMS film was attached to the glass plates. To fabricate the active smart window, a PDMS film was attached to one glass plate as the substrate for PAH. After irradiation with a UV lamp (22 mW cm^{-2} broadband light with a maximum peak at 365 nm; Jelight) for 4 h, the precursor solution was cross-linked into PAH. A PAH layer or a PAH/PDMS layer was peeled off from the glass plates, and dialyzed in a large bath of deionized (DI) water for 12 h.

PAH Sample Characterization. A custom-made laser measurement system was used to characterize PAH. A focus adjustable laser diode module (635 nm, 4.5 mW, CPS635F, Thorlabs) was employed as the light source. Two photodiodes (PDB-C160SM, Luna Optoelectronics) connected to the data acquisition device (USB-6009, National Instruments) were installed at 0° and 75° to the laser beam axis to acquire the transmitted light and scattered light, respectively. PAH samples (0.5 mm thickness) were kept in the temperature-control unit with 0.2 mm CaF_2 windows (TS102G, Instec Inc.) during the measurement. For the static temperature tests, samples were stabilized at the desired temperatures for 10 min before measurement. For the dynamic temperature tests, the signals were continuously acquired under programmed heating and cooling cycles between 15 and 65 °C at the ramping rates of ±5, ±10, and ±20 °C/min, respectively. The UV−vis transmittance spectra of PAH samples (0.5 mm thickness) were obtained on a NIR−UV spectrophotometer (PerkinElmer). The IR transmittance spectra were obtained on a Fourier transform infrared spectrophotometer (FTIR, Nicolet 8700, Thermo) with the temperature-control unit. In both UV−vis and FTIR measurements, samples were held at the desired temperature for 10 min before the measurement and the spectra upon heating were acquired. For the SEM sample preparation, two pieces of PAH-03 samples were kept at 20 and 55 °C on the hot plate for 5 min, and quenched in the liquid nitrogen immediately, followed by freeze-drying in the freeze-dryer (Super Modulyo, Savant). The water content of PAH was calculated on the basis of the mass difference of pristine samples and freeze-dried samples. The morphologies of freeze-dried samples were sputter coated (Denton) with 10 nm of gold and investigated by field emission SEM (Sigma, Zeiss) at 5 kV.

Fabrication of an Active Array of Temperature-Responsive Smart Window. The array of heaters was directly printed with our developed elastic conductive ink[39] by using a 3D jet printer (Tabletop 3Dn, nScrypt) with a nozzle diameter of 200 μm. The printed heater trace was 250 μm in width with thickness ranging between 27 and 30 μm. After printing, the conductive traces were annealed at 110 °C for 2 h to evaporate any remaining solvent (methyl isobutyl ketone) in the trace. We designed several patterns of the array (see Figure S3, Supporting Information).

Operation and Characterization of the Smart Window. Direct current with controlled function forms was generated by a Keithley 2400A source meter unit. Applied current and heater resistance were synchronously measured during the operation. A smartphone-attachable infrared camera (Compact, SEEK Thermal Inc.) was used for thermal imaging of the device. A digital camera was also used to capture the evolution of optical properties concurrently with the thermal imaging.

Spherical Radius Determination of the Water-Rich Domain. The spherical diameter of the water-rich domain was determined by relating it to the normalized scattering intensity, which was measured by our lab-made laser scattering measurement system for a wavelength λ = 635 nm at scattering angle θ = 75°. From eq 1, the formula of the normalized scattering intensity is obtained as $\overline{I_{sca}} = \overline{i_1} + \overline{i_2}$. As the normalized intensity functions $\overline{i_1}$ and $\overline{i_2}$ depend on the spherical radius r, we solved $\overline{i_1}$ and $\overline{i_2}$ as the infinite series for r (see in Supporting Information). In our calculation, the refractive index of the PAH-03 is 1.3333, and the refractive index of air is 1.0003. MATLAB scripts were programmed to solve the infinite series.

ASSOCIATED CONTENT

Supporting Information

The Supporting Information is available free of charge via the Internet at The Supporting Information is available free of charge on the ACS Publications website at DOI: 10.1021/acsami.7b08907.

Detailed experimental procedure and characterization method, theoretical model and analysis, and printing fabrication (PDF)

Video showing operation of the smart window (AVI)

Video demonstrating optical transparency (AVI)

Video demonstrating thermal transparency (AVI)

AUTHOR INFORMATION

Corresponding Author

*E-mail: chung.hj13@ualberta.ca.

ORCID

Thanh-Giang La: 0000-0001-7671-3726

Xinda Li: 0000-0003-0670-8651

Shu Yang: 0000-0001-8834-3320

Hyun-Joong Chung: 0000-0003-0569-6951

Author Contributions

#The manuscript was written through contributions of all authors. All authors have given approval to the final version of the manuscript. T.-G.L. and X.L. contributed equally.

Notes

The authors declare no competing financial interest.

ACKNOWLEDGMENTS

This work was financially supported by Natural Sciences and Engineering Research Council of Canada (NSERC; RGPIN 435914). XL acknowledges the support from Alberta Innovates through Doctoral Scholarship Program.

REFERENCES

(1) Bechinger, C.; Ferrere, S.; Zaban, A.; Sprague, J.; Gregg, B. A. Photoelectrochromic Windows and Displays. *Nature* **1996**, *383*, 608−610.

(2) Granqvist, C. G. Electrochromics for smart windows: Oxide-based thin films and devices. *Thin Solid Films* **2014**, *564*, 1−38.

(3) Wang, Y.; Runnerstrom, E. L.; Milliron, D. J. Switchable Materials for Smart Windows. *Annu. Rev. Chem. Biomol. Eng.* **2016**, *7*, 283−304.

(4) Gomez-Romero, P. Hybrid Organic-Inorganic Materials - In Search of Synergic Activity. *Adv. Mater.* **2001**, *13*, 163−174.

(5) Granqvist, C. G.; Azens, A.; Hjelm, A.; Kullman, L.; Niklasson, G. A.; Ronnow, D.; Mattsson, M. S.; Veszelei, M.; Vaivars, G. Recent Advances in Electrochromics for Smart Windows Applications. *Sol. Energy* **1998**, *63*, 199−216.

(6) Jensen, J.; Krebs, F. C. From the Bottom Up - Flexible Solid State Electrochromic Devices. *Adv. Mater.* **2014**, *26*, 7231−7234.

DOI: 10.1021/acsami.7b08907
ACS Appl. Mater. Interfaces 2017, 9, 33100−33106

(7) Babulanam, S. M.; Eriksson, T. S.; Niklasson, G. A.; Granqvist, C. G. Thermochromic VO_2 Films for Energy-Efficient Windows. *Sol. Energy Mater.* **1987**, *16*, 347−363.
(8) Lu, N.; Zhang, P.; Zhang, Q.; Qiao, R.; He, Q.; et al. Electric-Field Control of Tri-State Phase Transformation with a Selective Dual-Ion Switch. *Nature* **2017**, *546*, 124.
(9) Wang, N.; Duchamp, M.; Dunin-Borkowski, R. E.; Liu, S.; Zeng, X. T.; Cao, X.; Long, Y. Terbium-Doped VO2 Thin Films: Reduced Phase Transition Temperature and Largely Enhanced Luminous Transmittance. *Langmuir* **2016**, *32*, 759−764.
(10) Granqvist, C. G. Electrochromic Oxides - Systematics, Materials, and Applications to Smart Windows. *Renewable Energy* **1994**, *5*, 141−153.
(11) Chen, Z.; Gao, Y.; Kang, L.; Cao, C.; Chen, S.; Luo, H. Fine Crystalline VO2 Nanoparticles: Synthesis, Abnormal Phase Transition Temperatures and Excellent Optical Properties of a Derived VO_2 Nanocomposite Foil. *J. Mater. Chem. A* **2014**, *2*, 2718−2727.
(12) Kim, H.; Kim, Y.; Kim, K. S.; Jeong, H. Y.; Jang, A. R.; Han, S. H.; Yoon, D. H.; Suh, K. S.; Shin, H. S.; Kim, T.; Yang, W. S. Flexible Thermochromic Window Based on Hybridized VO2/Graphene. *ACS Nano* **2013**, *7*, 5769−5776.
(13) Patil, R. A.; Devan, R. S.; Liou, Y.; Ma, Y. R. Efficient Electrochromic Smart Windows of One-Dimensional Pure Brookite TiO2 Nanoneedles. *Sol. Energy Mater. Sol. Cells* **2016**, *147*, 240−245.
(14) Laurenti, M.; Bianco, S.; Castellino, M.; Garino, N.; Virga, A.; Pirri, C. F.; Mandracci, P. Toward Plastic Smart Windows: Optimization of Indium Tin Oxide Electrodes for the Synthesis of Electrochromic Devices on Polycarbonate Substrates. *ACS Appl. Mater. Interfaces* **2016**, *8* (12), 8032−8042.
(15) Ge, D.; Lee, E.; Yang, L.; Cho, Y.; Li, M.; Gianola, D. S.; Yang, S. A Robust Smart Window: Reversibly Switching from High Transparency to Angle-Independent Structural Color Display. *Adv. Mater.* **2015**, *27* (15), 2489−2495.
(16) López Jiménez, F.; Kumar, S.; Reis, P. M. Soft Color Composites with Tunable Optical Transmittance. *Adv. Opt. Mater.* **2016**, *4* (4), 620−626.
(17) Yao, X.; Hu, Y.; Grinthal, A.; Wong, T.-S.; Mahadevan, L.; Aizenberg, J. Adaptive Fluid-Infused Porous Films with Tunable Transparency and Wettability. *Nat. Mater.* **2013**, *12* (6), 529−534.
(18) Zhou, Y.; Cai, Y.; Hu, X.; Long, Y. Temperature-Responsive Hydrogel with Ultra-Large Solar Modulation and High Luminous Transmission for "Smart Window" Applications. *J. Mater. Chem. A* **2014**, *2* (33), 13550−13555.
(19) Yang, Y.-S.; Zhou, Y.; Chiang, F. B. Y.; Long, Y. Temperature-Responsive Hydroxypropylcellulose Based Thermochromic Material and Its Smart Window Application. *RSC Adv.* **2016**, *6*, 61449.
(20) Liu, J.; An, T.; Chen, Z.; Wang, Z.; Zhou, H.; Fan, T.; Zhang, D.; Antonietti, M. Carbon Nitride Nanosheets as Visible Light Photocatalytic Initiators and Crosslinkers for Hydrogels with Thermoresponsive Turbidity. *J. Mater. Chem. A* **2017**, *5*, 8933.
(21) Zhou, Y.; Layani, M.; Boey, F. Y. C.; Sokolov, I.; Magdassi, S.; Long, Y. Electro-Thermochromic Devices Composed of Self-Assembled Transparent Electrodes and Hydrogels. *Adv. Mater. Technol.* **2016**, *1* (5), 1600069.
(22) Owusu-Nkwantabisah, S.; Gillmor, J.; Switalski, S.; Mis, M. R.; Bennett, G.; Moody, R.; Antalek, B.; Gutierrez, R.; Slater, G. Synergistic Thermoresponsive Optical Properties of a Composite Self-Healing Hydrogel. *Macromolecules* **2017**, *50* (9), 3671−3679.
(23) Haraguchi, K. Nanocomposite Hydrogels. *Curr. Opin. Solid State Mater. Sci.* **2007**, *11* (3), 47−54.
(24) Sun, J.-Y.; Zhao, X.; Illeperuma, W. R.; Chaudhuri, O.; Oh, K. H.; Mooney, D. J.; Vlassak, J. J.; Suo, Z. Highly Stretchable and Tough Hydrogels. *Nature* **2012**, *489* (7414), 133−136.
(25) Haque, M. A.; Kurokawa, T.; Gong, J. P. Super Tough Double Network Hydrogels and Their Application as Biomaterials. *Polymer* **2012**, *53* (9), 1805−1822.
(26) Keplinger, C.; Sun, J.-Y.; Foo, C. C.; Rothemund, P.; Whitesides, G. M.; Suo, Z. Stretchable, Transparent, Ionic Conductors. *Science* **2013**, *341* (6149), 984−987.
(27) Zhao, X. Multi-Scale Multi-Mechanism Design of Tough Hydrogels: Building Dissipation into Stretchy Networks. *Soft Matter* **2014**, *10* (5), 672−687.
(28) Sun, T. L.; Kurokawa, T.; Kuroda, S.; Ihsan, A. B.; Akasaki, T.; Sato, K.; Haque, M. A.; Nakajima, T.; Gong, J. P. Physical Hydrogels Composed of Polyampholytes Demonstrate High Toughness and Viscoelasticity. *Nat. Mater.* **2013**, *12* (10), 932−937.
(29) Zhou, G.; Luo, J.; Liu, C.; Chu, L.; Ma, J.; Tang, Y.; Zeng, Z.; Luo, S. A highly Efficient Polyampholyte Hydrogel Sorbent Based Fixed-Bed Process for Heavy Metal Removal in Actual Industrial Effluent. *Water Res.* **2016**, *89*, 151−160.
(30) Wei, Z.; Yang, J. H.; Zhou, J.; Xu, F.; Zrinyi, M.; Dussault, P. H.; Osada, Y.; Chen, Y. M. Self-Healing Gels Based on Constitutional Dynamic Chemistry and Their Potential Applications. *Chem. Soc. Rev.* **2014**, *43* (23), 8114−8131.
(31) Li, X.; Liu, L.; Wang, X.; Ok, Y. S.; Elliott, J. A. W.; Chang, S. X.; Chung, H.-J. Flexible and Self-Healing Aqueous Supercapacitors for Low Temperature Applications: Polyampholyte Gel Electrolytes with Biochar Electrodes. *Sci. Rep.* **2017**, *7*, 1685.
(32) Ihsan, A. B.; Sun, T. L.; Kurokawa, T.; Karobi, S. N.; Nakajima, T.; Nonoyama, T.; Roy, C. K.; Luo, F.; Gong, J. P. Self-Healing Behaviors of Tough Polyampholyte Hydrogels. *Macromolecules* **2016**, *49* (11), 4245−4252.
(33) Givoni, B. *Passive Low Energy Cooling of Buildings*; John Wiley & Sons, 1994.
(34) Bella, F.; Leftheriotis, G.; Griffini, G.; Syrrokostas, G.; Turri, S.; Gratzel, M.; Gerbaldi, C. A New Design Paradigm for Smart Windows: Photocurable Polymers for Quasi-Solid Photoelectrochromic Devices with Excellent Long-Term Stability under Real Outdoor Operating Conditions. *Adv. Funct. Mater.* **2016**, *26* (7), 1127−1137.
(35) Seuring, J.; Bayer, F. M.; Huber, K.; Agarwal, S. Upper Critical Solution Temperature of Poly(N-acryloyl glycinamide) in Water: A Concealed Property. *Macromolecules* **2012**, *45* (1), 374−384.
(36) Seuring, J.; Agarwal, S. Polymers with Upper Critical Solution Temperature in Aqueous Solution. *Macromol. Rapid Commun.* **2012**, *33* (22), 1898−1920.
(37) Woodfield, P. A.; Zhu, Y.; Pei, Y.; Roth, P. J. Hydrophobically Modified Sulfobetaine Copolymers with Tunable Aqueous UCST through Postpolymerization Modification of Poly(pentafluorophenyl acrylate). *Macromolecules* **2014**, *47* (2), 750−762.
(38) Wiscombe, J. Mie Scattering Calculations: Advances in Technique and Fast, Vector-Speed Computer Codes. *NCAR Technical Note NCAR/TN-140+STR*; National Center for Atmospheric Research, 1979; DOI: 10.5065/D6ZP4414.
(39) Kumar, H. S.; La, T. G.; Honari, M. M.; Charaya, H.; Damis, H. A.; Mousavi, P.; Chung, H. J. A Highly Deformable Conductive Ink of Silver/Fluoropolymer Based Composite Compatibilzed by with Ag Particles as 3D Printable Conductive Ink for Stretchable Electronics. *Flex. Print. Electron.*, in revision.
(40) Yuk, H.; Zhang, T.; Parada, G. A.; Liu, X.; Zhao, X. Skin-Inspired Hydrogel−Elastomer Hybrids with Robust Interfaces and Functional Microstructures. *Nat. Commun.* **2016**, *7*, 12028.
(41) Zang, J.; Ryu, S.; Pugno, N.; Wang, Q.; Tu, Q.; Buehler, M. J.; Zhao, X. Multifunctionality and Control of the Crumpling and Unfolding of Large-Area Graphene. *Nat. Mater.* **2013**, *12* (4), 321−325.
(42) Sun, J. Y.; Keplinger, C.; Whitesides, G. M.; Suo, Z. Ionic Skin. *Adv. Mater.* **2014**, *26* (45), 7608−7614.
(43) Cha, C.; Antoniadou, E.; Lee, M.; Jeong, J. H.; Ahmed, W. W.; Saif, T. A.; Boppart, S. A.; Kong, H. Tailoring Hydrogel Adhesion to Polydimethylsiloxane Substrates Using Polysaccharide Glue. *Angew. Chem., Int. Ed.* **2013**, *52* (27), 6949−6952.
(44) Yuk, H.; Zhang, T.; Lin, S.; Parada, G. A.; Zhao, X. Tough Bonding of Hydrogels to Diverse Non-Porous Surfaces. *Nat. Mater.* **2016**, *15* (2), 190−196.

DOI: 10.1021/acsami.7b08907
ACS Appl. Mater. Interfaces 2017, 9, 33100−33106

SUPPORTING INFORMATION FOR:

Highly Flexible, Multi-Pixelated Thermochromic Smart Windows Made of Tough Hydrogels

Thanh-Giang La, [†,‡,¶,‖] Xinda Li,[†,‖] Amit Kumar, [†] Yiyang Fu,[ᵀ] Shu Yang,[§] and Hyun-Joong Chung*[,†]

[†]Department of Chemical and Materials Engineering, University of Alberta, Edmonton, Alberta T6G1H9, Canada

[‡]Institute for Reconstructive Sciences in Medicine (iRSM), Misericordia Community Hospital, Edmonton, Alberta T5R4H5, Canada

[¶]Department of Communication Sciences and Disorders, University of Alberta, Edmonton, Alberta T6G2G4, Canada

[ᵀ]Department of Electrical and Computer Engineering, University of Alberta, Edmonton, Alberta T6G1H9, Canada

[§]Department of Materials Science and Engineering, University of Pennsylvania, Philadelphia, Pennsylvania 19104, United States

KEYWORDS: tough hydrogels, smart windows, optical coating, stretchable electronics, phase separation

*Address correspondences to chung.hj13@ualberta.ca

[‖]These authors contributed equally.

Laser scattering intensity measurement

The scattering intensity was known as $I_{scat} = I_o(1/r^2)\sigma'_{scat}$ where σ_{scat} is the scattering cross section. As following Mie's theory [S1], the differential scattering cross section can be determined as $\sigma'_{scat} = \lambda^2(i_1 + i_2)/(8\pi^2)$ where,

$$i_1 = \left|\sum_{n=1}^{\infty} \frac{2n+1}{n(n+1)} [a_n \pi_n(\cos\theta) + b_n \tau_n(\sin\theta)]\right|^2, \quad \text{(S1)}$$

$$i_2 = \left|\sum_{n=1}^{\infty} \frac{2n+1}{n(n+1)} [a_n \tau_n(\cos\theta) + b_n \pi_n(\sin\theta)]\right|^2. \quad \text{(S2)}$$

with a_n and b_n are expressed as Ricatti-Bessel functions depended on the size parameter $\alpha = 2\pi r/\lambda$; and π_n and τ_n are the angular dependent functions. The infinite series i_1 and i_2 can be solved by Matlab programming numerically.

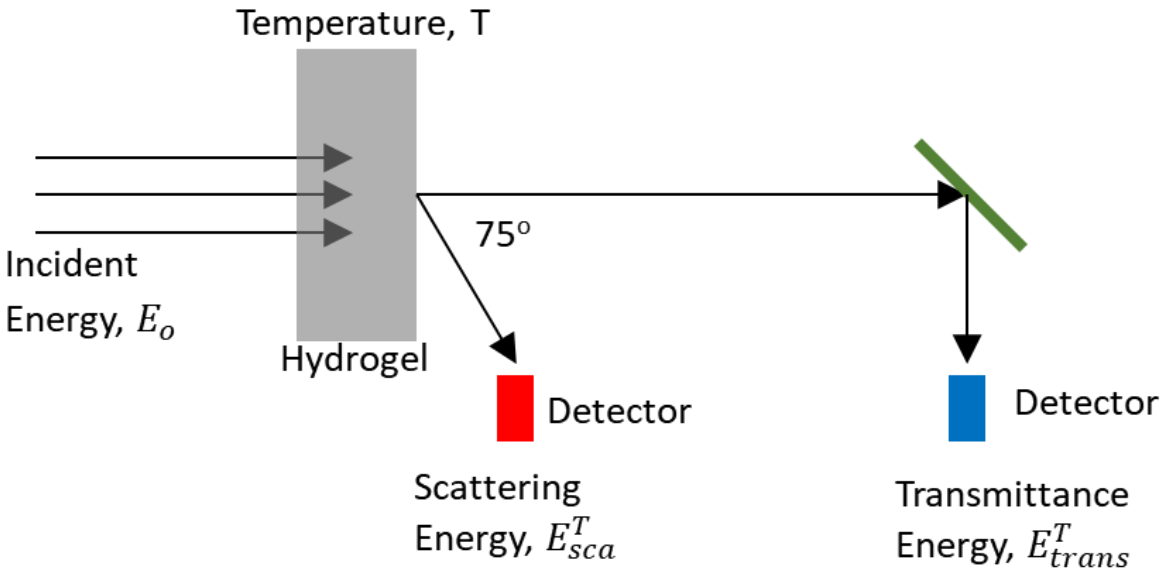

Figure S1. Setup of Laser Light Scattering Intensity Measurement. Temperature of PAH with thickness of 500um was controlled from 10 to 70 °C in an interval of 5 °C.

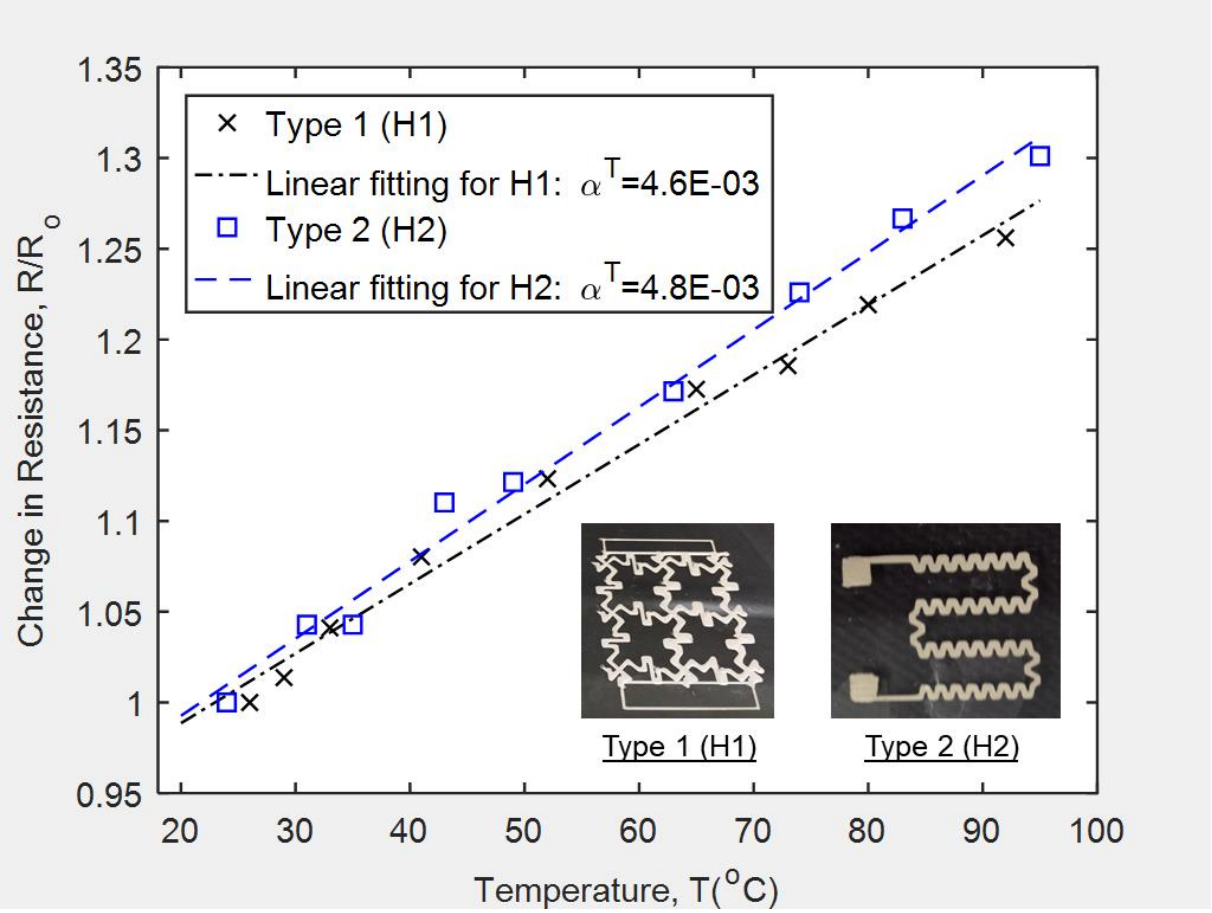

Figure S2. Temperature dependent resistance of stretchable heaters. Temperature coefficient of resistance α^T was determined by fitting the temperature-resistance curves linearly, as $R/R_o = 1 + \alpha^T(T - T_o)$ where R_o is the initial resistance at room temperature T_o, and R is the resistance at elevated temperature T.

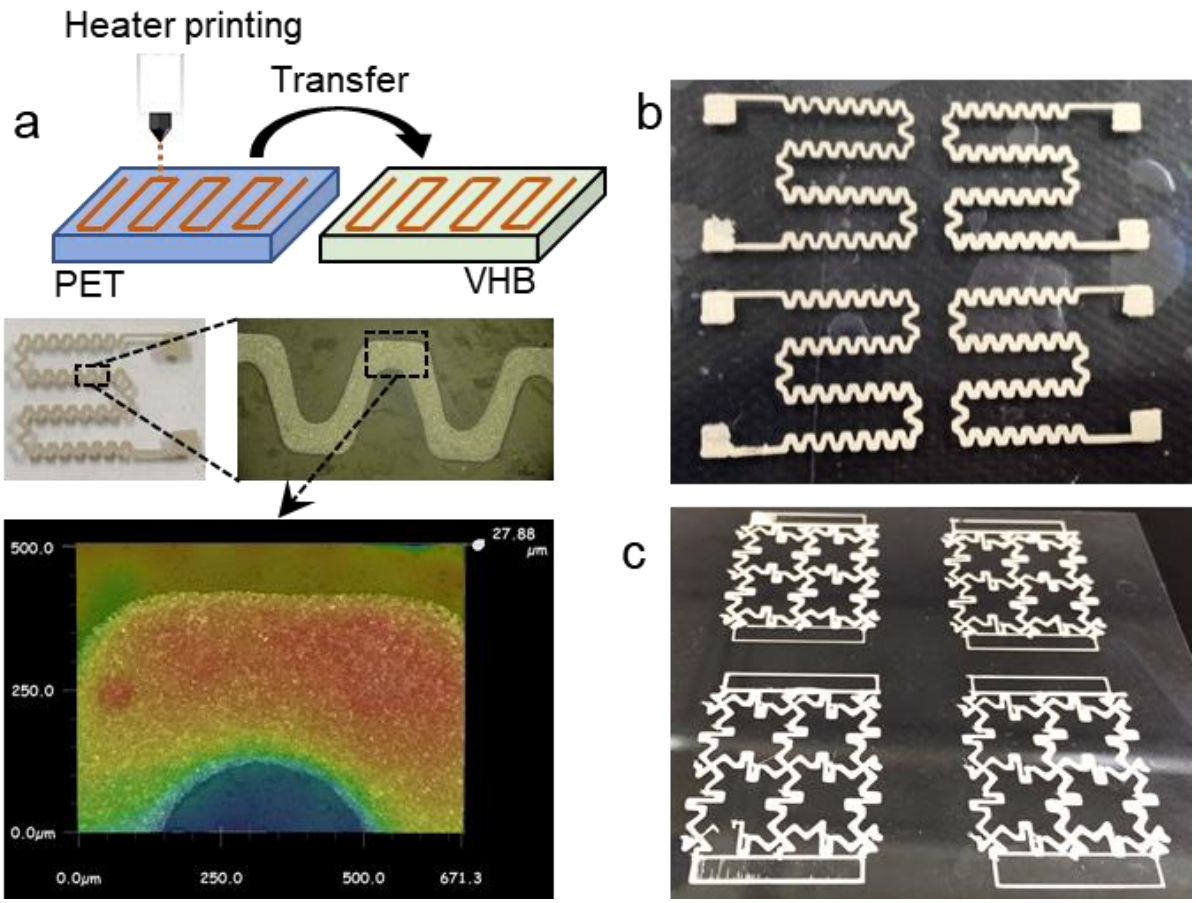

Figure S3. Design and fabrication of the stretchable heater array. (a) Schematic of jet-printing of the heater array on PET and transferring it to VHB substrate; and optical photographs and microscopy images. (b) and (c) Two different designs of the stretchable heater array.

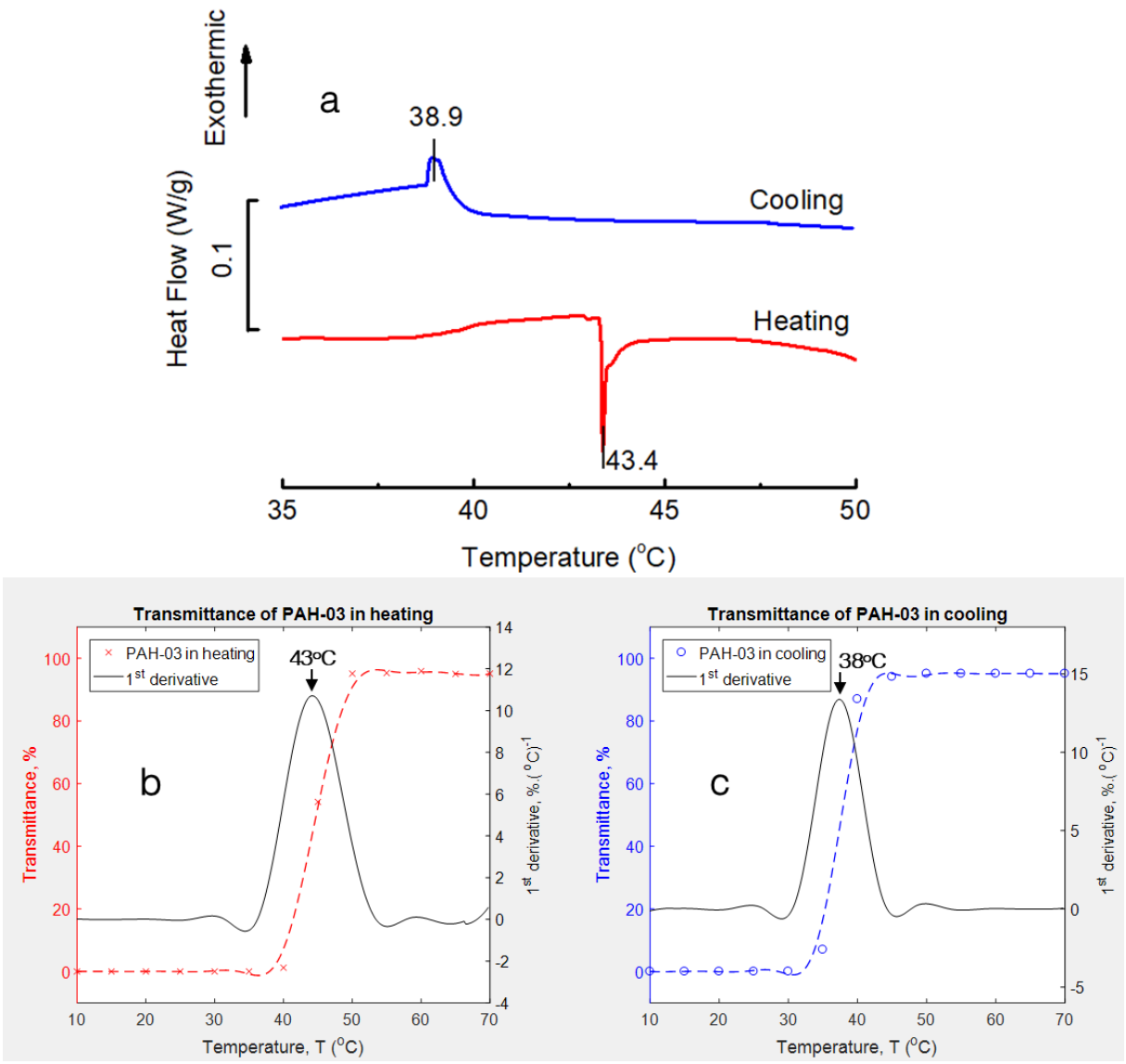

Figure S4. (a) Differential scanning calorimetry (DSC) for the PAH-03 in heating and cooling between 15 °C and 65 °C at the ramping rate of 5 °C/min. Transmittance vs. temperature curves and their 1st derivatives of the PAH-03 in (b) heating, and (c) cooling.

The total monomer conversion rate was determined by 1H NMR. The NMR spectra were acquired on the Agilent VNMRS V700 operating at 699.7 MHz at room temperature. The sample preparation was described as following: as-prepared PAH-003 was weighted and dissolved in 4 M NaCl deuterium oxide solution overnight. The same amount of precursor solution for PAH-003 was also diluted in the NaCl deuterium oxide solution. Weighted DSS (4,4-dimethyl-4-silapentane-1-sulfonic acid sodium salt) was added into both solution as the internal standard substitute. The monomer conversion rate was determined by comparing the integrated peak area in the range of 7 to 5.5 ppm, which are proton signals from the alkene groups in the monomers (NaSS, MPTC, DAC, and MBAA). The intensity of peaks were normalized by most intensive signal from DSS labelled by 1 in both spectra. No obvious peak was observed in PAH-003 spectrum, indicating the complete conversion after the polymerization.

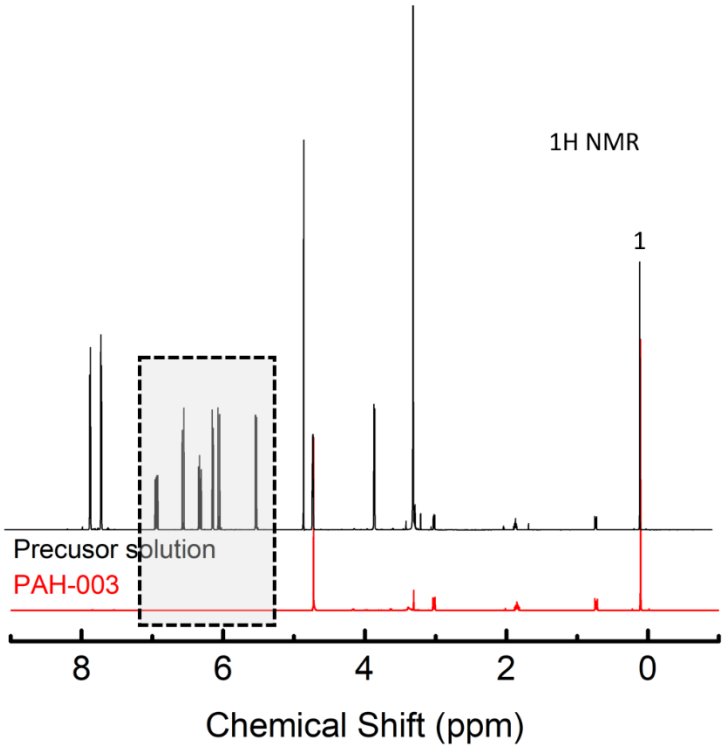

Figure S5. 1H-NMR spectra of the PAH-03 and the precursor solution (including the monomers NaSS, MPTC, DAC, and MBAA) at room temperature.

Table S1. Time response of electrochromic and thermochromic smart windows.

Switching mechanism	Chromic Material	Response time	Reference
Electrochromism	WO_3	90 s / half cycle	Bella et al. 2016 [S2]
Electrochromism	Prussian blue/ ZnHCF	~ 150 s / cycle	Yeh et al. 2015 [S3]
Electrochromism	EControl Glass*	15 – 20 mins / cycle	Wang et al. 2016 [S4]
Electrochromism	WO_3	~ 400 s / cycle	Bechinger et al. 1996 [S5]
Thermochromism (Phase-separation)	PNIPAm hydrogel	~ 300 s / cycle	Zhou et al. 2016 [S6]
Thermochromism (Phase-separation)	PNIPAm hydrogel (dispersed as nanogels)	30 s / half cycle	Owusu-Nkwantabisah et al. 2017 [S7]
Thermochromism (Phase-separation)	PAH	~70 s / cycle	Our study

*a commercial product of EControl Glass GmbH (Ref [S4]).

Supplementary Video S1.

This movie shows transparent control of the PAH-based window.

Supplementary Video S2.

This movie shows transparent pixelated-control of the PAH-based window.

Supplementary Video S3.

This movie shows infrared thermal video of the heater array upon pixelated control (taken from the heater side).

REFERENCES

S1. Wiscombe, J., Mie scattering calculations: Advances in technique and fast, vector-speed computer codes. **1979**.

S2. Bella, F.; Leftheriotis, G.; Griffini, G.; Syrrokostas, G.; Turri, S.; Gratzel, M.; Gerbaldi, C., A New Design Paradigm for Smart Windows: Photocurable Polymers for Quasi-Solid Photoelectrochromic Devices with Excellent Long-Term Stability under Real Outdoor Operating Conditions. *Adv Funct Mater* **2016,** *26* (7), 1127-1137.

S3. Yeh, M. H.; Lin, L.; Yang, P. K.; Wang, Z. L., Motion-Driven Electrochromic Reactions for Self-Powered Smart Window System. *Acs Nano* **2015,** *9* (5), 4757-4765.

S4. Wang, Y.; Runnerstrom, E. L.; Milliron, D. J., Switchable Materials for Smart Windows. *Annu Rev Chem Biomol* **2016,** *7*, 283-304.

S5. Bechinger, C.; Ferrer, S.; Zaban, A.; Sprague, J.; Gregg, B. A., Photoelectrochromic windows and displays. *Nature* **1996,** *383* (6601), 608-610.

S6. Zhou, Y.; Layani, M.; Boey, F. Y. C.; Sokolov, I.; Magdassi, S.; Long, Y., Electro-Thermochromic Devices Composed of Self-Assembled Transparent Electrodes and Hydrogels. *Advanced Materials Technologies* **2016,** *1* (5), 1600069.

S7. Owusu-Nkwantabisah, S.; Gillmor, J.; Switalski, S.; Mis, M. R.; Bennett, G.; Moody, R.; Antalek, B.; Gutierrez, R; Slater, G., Synergistic Thermoresponsive Optical Properties of a Composite Self-Healing Hydrogel. *Macromolecules* **2017**, *50*, 3671-3679.